Nature of weak inter- and intramolecular interactions in crystals
4.* Bifurcated N—H...N bond in a crystal of 3-amino-6-(3,5-dimethylpyrazol-1-yl)-1,2,4,5-tetrazine**

K. A. Lyssenko,[a]★ D. V. Lyubetsky,[a] A. B. Sheremetev,[b] and M. Yu. Antipin[a]

[a]*A. N. Nesmeyanov Institute of Organoelement Compounds, Russian Academy of Sciences, 28 ul. Vavilova, 119991 Moscow, Russian Federation. Fax: +7 (095) 135 5085. E-mail: kostya@xray.ineos.ac.ru*
[b]*N. D. Zelinsky Institute of Organic Chemistry, Russian Academy of Sciences, 47 Leninsky prosp., 119991 Moscow, Russian Federation. Fax: +7 (095) 135 5328*

The nature and the energy of the intermolecular bifurcated N—H...N hydrogen bond in the crystal of 3-amino-6-(3,5-dimethylpyrazol-1-yl)-1,2,4,5-tetrazine were studied by analyzing the electron density distribution based on X-ray diffraction data. In contrast to two-center hydrogen bonds, the total energy of the N—H...N interaction is virtually independent of the geometric parameters of two contacts and is determined only by the nature of the interacting atoms.

Key words: tetrazines, bifurcated H bonds, stacking interaction, electron density distribution, topological theory of Atoms in Molecules, X-ray diffraction.

Hydrogen bonds occupy a prominent place among a variety of chemical interactions due, primarily, to their great role in various biochemical processes.[2] Reliable experimental methods have been developed for studying hydrogen bonds of various nature and estimating their energy. Spectroscopic methods, such as IR and Raman spectroscopy, take the leading position. These methods allow one not only to evaluate the energies of interactions but also to elucidate the proton transfer mechanism.[3] Conventional X-ray and neutron diffraction studies provide primarily a "visual information"[4] because the presence of shortened interatomic distances and the directionality of contacts not always allow unambiguous conclusions about hydrogen bonding, as well as about the formation of any other specific interaction (see Ref. 1). Therefore, diffraction and spectroscopic methods essentially supplement each other and enable one to study various systems with inter- and intramolecular hydrogen bonds.

However, spectroscopic methods and conventional X-ray diffraction studies, as well as their combinations, as applied to the solution of certain problems give no results. This refers to studies of unsymmetrical bifurcated H bonds. In the latter case, spectroscopic methods only give evidence for the presence of hydrogen bonding, but do not allow one to distinguish whether the hydrogen atom is involved in one or two hydrogen bonds. X-ray diffraction studies, in turn, provide information only about interatomic distances and do not enable one to distinguish bifurcated and usual two-center interactions.

The topological analysis of the experimental electron density distribution function $\rho(\mathbf{r})$ in crystals in terms of Bader's theory "Atoms in Molecules" (AIM)[5] is the only experimental method for studying bifurcated H bonds, which gives exhaustive information on the nature and energy of these interactions. This approach is of particular interest because it allows one not only to distinguish attractive interactions from a totality of contacts but also to estimate their energies E_{cont} from the semiquantitative dependence on the potential energy density, $v(\mathbf{r})$, at the bond critical point (3,−1).[6]

Earlier,[7] topological investigations of $\rho(\mathbf{r})$ for bifurcated H bonds have been carried out only based on the results of quantum-chemical calculations, whereas studies of unsymmetrical bifurcated H bonds in crystals are virtually lacking and have been limited to analysis of weak C—H...O interactions (H...O distances are approximately equal to 2.4 Å).[8,9]

Since the strength of hydrogen bonds depends on the polarity of the medium and specific solvation, which are difficult and sometimes impossible to take into account in quantum-chemical calculations, it was of interest to perform an experimental investigation of bifurcated H bonds

* For Part 3, see Ref. 1.

** Dedicated to Academician V. I. Minkin on the occasion of his 70th birthday.

Published in Russian in *Izvestiya Akademii Nauk. Seriya Khimicheskaya,* No. 4, pp. 903—910, April, 2005.

1066-5285/05/5404-0924

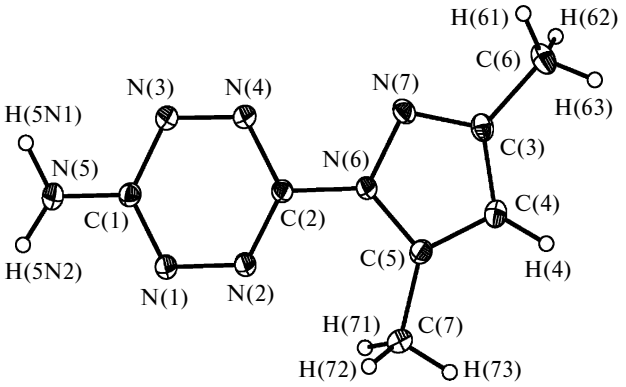

Fig. 1. Overall view of compound **1** with displacement ellipsoids drawn at the 50% probability level.

in crystals, which, in part, simulate specific features of interactions in solution. We chose 3-amino-6-(3,5-dimethylpyrazol-1-yl)-1,2,4,5-tetrazine (**1**) (Fig. 1), whose crystals contain both usual two-center N—H...N bonds and rather strong bifurcated N—H...N bonds.

This class of compounds is also of interest because of their potentiality in the preparation of energetic materials. For example, it was reported[10] that 3,3′-azobis(6-amino-1,2,4,5-tetrazine) has an usually high density (1.84 g cm^{-3}), which is the maximum density for compounds consisting only of C, H, and N atoms.

Hence, studies of the character and energy of intermolecular contacts in the tetrazine series is not only of theoretical but also of applied interest for the design of energetic materials.

Results and Discussion

Molecular and crystal structure. Principal geometric parameters of molecule **1** are given in Table 1. The pyrazole ring is planar, whereas the tetrazine ring adopts a strongly flattened boat conformation with the C(1) and C(2) atoms deviating from the N(1)N(2)N(3)N(4) plane by 0.1228(8) and 0.0945(8) Å, respectively. The pyrazole and tetrazine rings are coplanar; the N(4)C(2)N(6)N(7) torsion angle (ϕ) is 0.2°. By contrast, the ϕ angle in the structure of related *N*,*N*″-bis[6-(3,5-dimethylpyrazol-1-yl)-1,2,4,5-tetrazin-3-yl]piperazine is 50°,[11] whereas this angle in 3,6-bis(pyridin-2-yl)-1,2,4,5-tetrazine[12] is 19°. Therefore, conjugation between the pyrazole and tetrazine rings is, apparently, absent and a decrease in the twist angle ϕ in **1** is attributable to the influence of intermolecular interactions. Actually, our quantum-chemical calculations at the B3LYP/6-311+G** level of theory demonstrated that the ϕ angle in the isolated molecule is 35°. It should be noted that, in spite of the fact that the twist angle in the crystal differs from that in the isolated molecule, the geometric parameters of the pyrazole ring (see Table 1), as well as the C(2)—N(6) bond length (1.403(1) and 1.400 Å, respectively), are virtually equal.

Table 1. Main geometric parameters of molecule **1** (bond lengths (*d*), bond angles (ω), and torsion angles (τ)) determined by X-ray diffraction study and quantum-chemical calculations

Parameter	X-ray diffraction	B3LYP/6-311+G**
Bond	*d*/Å	
N(1)—N(2)	1.330(1)	1.313
N(3)—N(4)	1.309(1)	1.305
C(1)—N(1)	1.353(1)	1.346
C(1)—N(3)	1.367(1)	1.353
C(1)—N(5)	1.338(1)	1.355
C(2)—N(4)	1.330(1)	1.343
C(2)—N(2)	1.346(1)	1.334
C(2)—N(6)	1.403(1)	1.400
N(6)—N(7)	1.379(1)	1.371
C(5)—N(6)	1.380(1)	1.383
C(3)—N(7)	1.328(1)	1.321
C(3)—C(4)	1.417(1)	1.423
C(4)—C(5)	1.378(1)	1.374
C(3)—C(6)	1.494(1)	1.496
C(5)—C(7)	1.486(1)	1.494
Angle	ω/deg	
N(5)—C(1)—N(1)	117.4(1)	118.2
N(1)—C(1)—N(3)	123.2(1)	124.3
N(2)—C(2)—N(4)	125.0(1)	124.8
C(2)—N(6)—N(7)	129.8(1)	129.1
C(4)—C(5)—C(7)	129.3(1)	129.7
C(3)—C(4)—C(5)	106.6(1)	106.3
C(4)—C(3)—C(6)	128.0(1)	128.3
C(3)—N(7)—N(6)	104.6(1)	105.1
	τ/deg	
N(5)—C(1)—N(1)—N(2)	−170.8(2)	−172.4
C(1)—N(1)—N(2)—C(2)	−1.9(2)	−2.7
C(1)—N(3)—N(4)—C(2)	0.7(2)	−1.5
N(2)—C(2)—N(6)—C(5)	−0.2(2)	32.4
C(2)—N(6)—C(5)—C(7)	2.0(2)	2.2
C(5)—C(4)—C(3)—N(7)	0.3(2)	−0.4

On the contrary, the geometry of the tetrazine ring in the crystal differs essentially from that in the isolated molecule. For example, the difference in the N—N bond lengths is 0.021(1) Å, whereas the N—C bond lengths vary from 1.330(1) to 1.367(1) Å. In the isolated molecule, the N—N and N—C bonds are equalized to a considerable extent (see Table 1). Analysis of CSD (Cambridge Structural Database)[13] information demonstrated that this nonequivalence of the N—N bond lengths is typical, primarily, of amino-substituted tetrazines. Apparently, alternation of the C—N and N—N bond lengths in the ring and a slight elongation of the C—N bonds at the C(1) atom compared to the corresponding bonds at the C(2) atom are attributable to a strong conjugation between the N(1)N(3)C(1) fragment and the NH_2 group, which is evident from shortening of the C(1)—N(5) bond

(1.338(1) Å) and flattening of the NH_2 group (sum of the angles at the N(5) atom is 359.5°). In the isolated molecule, the equalization of the bond lengths is associated with weakening of this conjugation, which is manifested in pyramidalization of the NH_2 group (sum of the angles at the N(5) angle is 355.5°) and elongation of the C(1)—N(5) bond (1.355 Å). The differences in the degree of conjugation, in turn, can be associated with the crystal packing effects. For example, the presence of H bonds formed by the amino group in the crystal results in an increase in the p character of the lone electron pair of the N(5) atom and, consequently, is favorable for conjugation with the tetrazine ring.

Actually, analysis of the crystal packing demonstrated that both hydrogen atoms of the amino group form medium-strength N—H...N hydrogen bonds (Table 2, Fig. 2, *a*). In the crystal, the molecules are linked by these bonds to form corrugated layers parallel to the crystallographic *bc* plane. In addition to the N—H...N bonds, the molecules in the layer are linked by weak C—H...N contacts (H...N, 2.49—2.51 Å) and stacking interactions between the atoms of the tetrazine and pyrazole rings with the following shortest distances: C...N, 3.302(1), 3.428(1) and 3.475(1) Å; C...C, 3.317(1) Å; N...N, 3.401(1) Å (see Table 2, Fig. 2, *b*). The contacts between the layers are substantially weaker than the contacts within the layer. Only C—H...N interactions (H...N, 2.56 Å) can be distinguished based on the geometric criteria.

The N—H...N bonds in the crystal differ substantially in length. The shortest H bond, through which molecules **1** are linked into the centrosymmetric dimer **A** (see Fig. 2, *a*), is formed by the H(5N(2)) atom and the N(1B) atom of the tetrazine ring (N...N, 3.139(1) Å). However, the bifurcated H bond formed by the H(5N(1)) atom with the N(4A) atom of the tetrazine ring and the N(7A) atom of the pyrazole ring (see Fig. 2) is of most interest. The components of this bonds differ substantially in strength, which is evident from the differences in the interatomic N...H (2.35 and 2.26 Å) and N...N distances (3.052(1) and 3.234(1) Å) and, primarily, in the N...H—N angles (126° and 163°) for the H bonds involving the N(4A) and N(7A) atoms, respectively. Therefore, in spite of the shorter N...N distance in the case of the H bond with the N(4A) atom, the N(5)—H(5N(1))...N(7A) angle is closer to 180°. The stronger H(5N(1))...N(7A) hydrogen bonding is also evidenced by the corresponding short N...H distance. However, it cannot be ruled out that the H(5N(1)) atom is involved only in one H bond (N(7A)...H—N), whereas the contact with the N(4A) atom is forced and is determined by the geometric features of the molecule (close arrangement of the N(4) and N(7) atoms).

Quantum-chemical calculations at the PBE/TZ2P//B3LYP/6-311+G** level of theory for the dimer **B**, in which molecules **1** are linked by the above-described bifurcated H bond, gave a larger difference in the N—H...N interactions of the bifurcated type (see Table 2). The N...N distances change inversely in going from the crystal to the isolated state: the N(5)...N(7A) contact is shortened (3.033 Å), whereas the N(5)....N(4A) contact is elongated (3.104 Å); the N(5)H(5N(1))N(7A) and N(5)H(5N(1))N(4A) angles also change to 175.2° and 106.2°, respectively. Hence, the differences in the geometric parameters and strength of interactions in the region of the bifurcated H bond become even larger in the isolated state.

Table 2. Geometric parameters of intermolecular contacts in the crystal of **1**

Fragment (symmetry code)	Distance/Å		Angle/deg A—H...B
	H...B[a]	A...B	
Interactions N—H....N			
N(5)—H(5N(2))...N(1) (1 − *x*, −*y*, −*z*)	2.15	3.139(1)	167
N(5)—H(5N(1))...N(4) (1 − *x*, −0.5 + *y*, 0.5 − *z*)	2.35/2.67[b]	3.052(1)/(3.104)[b]	126/(106.2)[b]
N(5)—H(5N(1))...N(7) (1 − *x*, −0.5 + *y*, 0.5 − *z*)	2.26/2.00[b]	3.234(1)/3.033)[b]	163/(175.2)[b]
Interactions C—H...N			
N(3)...H(61)—C(6) (1 − *x*, −0.5 + *y*, 0.5 − *z*)	2.49	3.499(1)	154
N(3)...H(72)—C(7) (*x*, 0.5 − *y*, 0.5 + *z*)	2.51	3.472(1)	148
N(2)...H(62)—C(6) (−*x*, 1 − *y*, −*z*)	2.56	3.448(1)	139
Stacking interactions[c]			
C(1)...C(4) (1 − *x*, 1 − *y*, −*z*)	—	3.317	—
C(5)...N(4) (1 − *x*, 1 − *y*, −*z*)	—	3.475	—

[a] The distance was calculated by the PBE/TZ2P//B3LYP/6-311+G** method for the dimer stabilized by the bifurcated N—H...N bond.

[b] The C—H bond lengths were normalized to the ideal distance (1.08 Å), and the N—H distances were evaluated by quantum-chemical calculations (B3LYP/6-311G**).

[c] For the stacking interactions, only contacts characterized by the critical points (3,−1) are given.

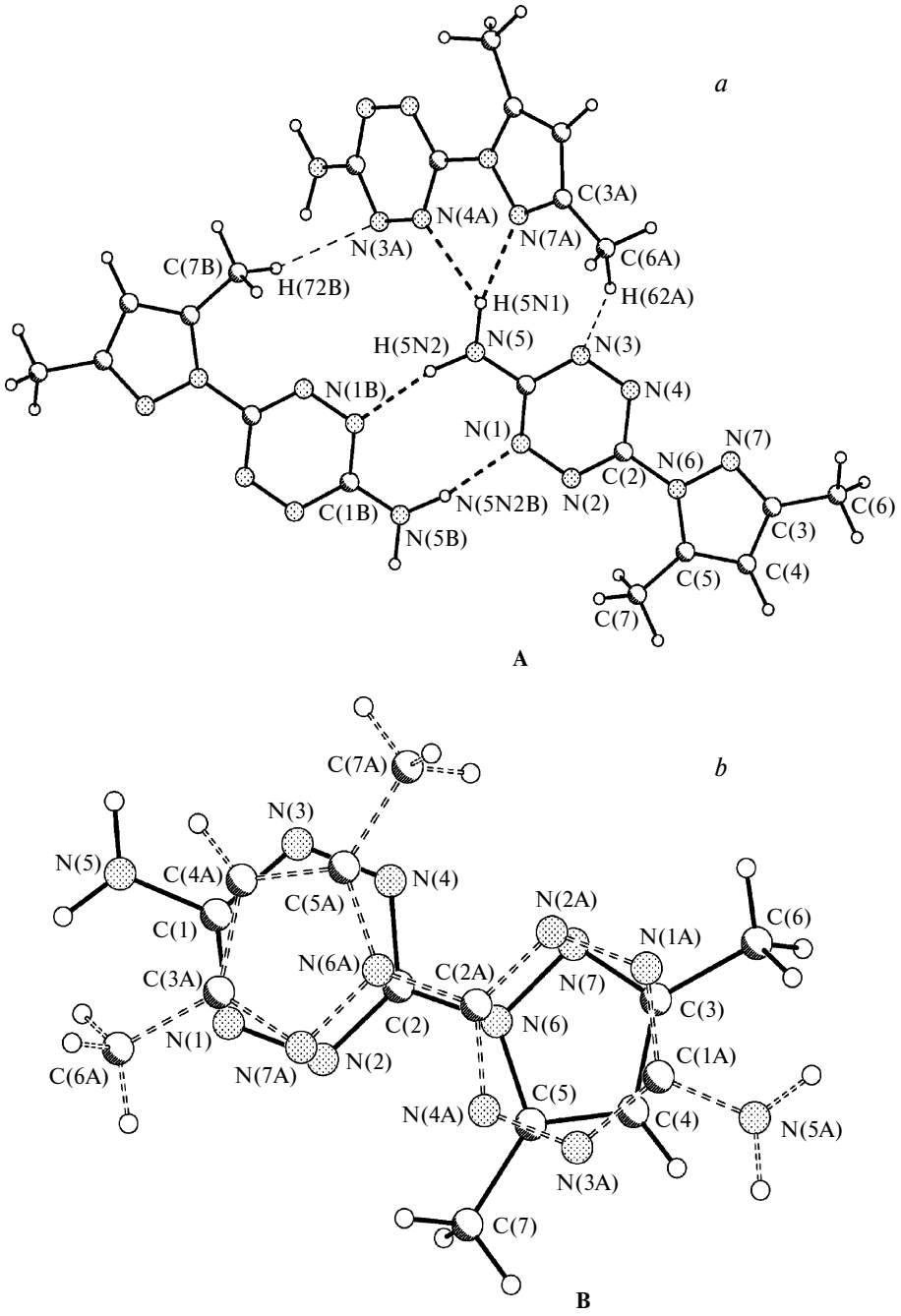

Fig. 2. Fragments of the layer in the crystal of **1** illustrating N—H...N hydrogen bonding, C—H.....N contacts (*a*), and stacking interactions (*b*).

To elucidate the character of the bifurcated N—H...N bond, stacking interactions, and weak C—H....N contacts and to evaluate their energy parameters, we carried out the topological analysis of the electron density distribution function $\rho(\mathbf{r})$ in the crystal of **1**, which was determined in the analytical form by the multipole refinement of X-ray diffraction data (see the Experimental section).

Topological analysis of the electron density distribution function. Before proceeding to the topological analysis of the electron density distribution, let us consider the characteristic features of the deformation electron density (DED) distribution in the molecule and also in the region of the N—H...N bonds in molecule **1**. The deformation electron density map (Fig. 3, *a*) in the rms plane of the tetrazine ring shows electron accumulation in all bonds, as well as in the vicinity of the lone electron pairs of the nitrogen atoms. The DED peaks in the N(1)—N(2) and N(3)—N(4) bonds are shifted toward the N(2) and N(3)

atoms, which is, apparently, associated with the effect of the amino group and the pyrazole substituent. An interesting feature of the deformation electron density distribution in the tetrazine ring is that the peaks are displaced from the N—N bond line toward the center of the ring. The presence of "bent bonds" in tetrazines has been observed earlier in a series of organic derivatives.[14] This fact was accounted for by the influence of the lone pairs of the nitrogen atoms, which push electron density from the N—N bond line toward the center of the ring. In contrast to the tetrazine ring, the DED peak in the N(6)—N(7) bond of the pyrazole ring (Fig. 3, *b*), in spite of the presence of the lone pair of the N(7) atom, is located in the N—N bond line. The peak in the N(6)—C(2) bond is shifted from the midpoint to the nitrogen atom, whereas the peak in the C(1)—N(5) bond is shifted to the carbon atom, which is in good agreement with the electron-withdrawing and electron-donating properties of the pyrazole ring and the amino group, respectively.

Analysis of the deformation electron density in the region of the N—H...N bonds demonstrated that the electron distribution in the centrosymmetric dimer is close to that expected for hydrogen bonding. The DED maxima in the N(5)—H(5N(2)) bond and in the region of the lone electron pair of the N(1B) atom are in a single line (Fig. 4, *a*). The difference in the peak heights corresponding to the lone pairs of the N(1) and N(2) atoms is

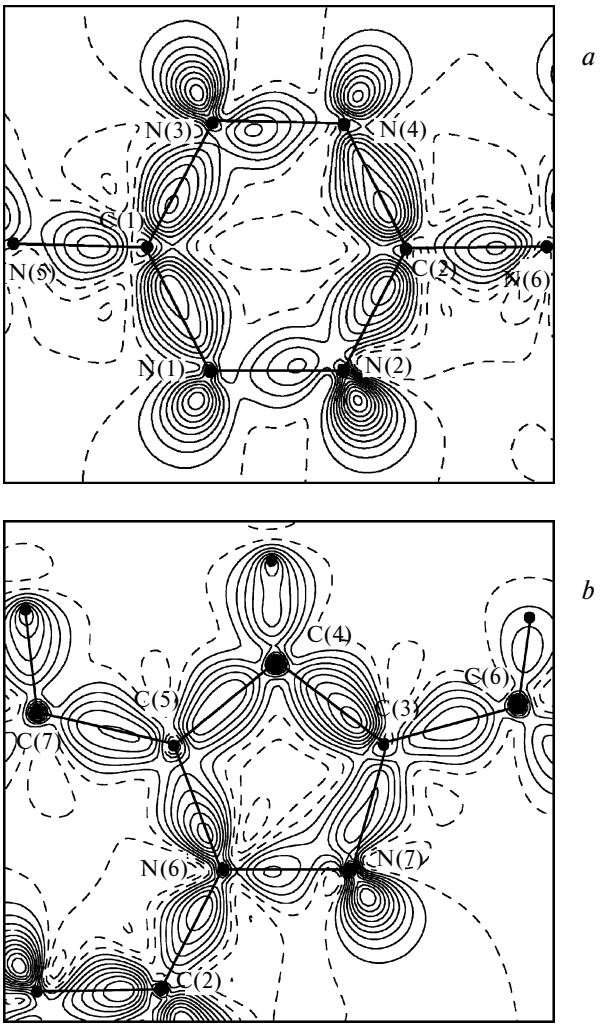

Fig. 3. Deformation electron density maps in the planes of the tetrazine (*a*) and pyrazole rings (*b*). The maps are contoured at 0.1 e Å^{-3} intervals. The negative and zero contours are dashed.

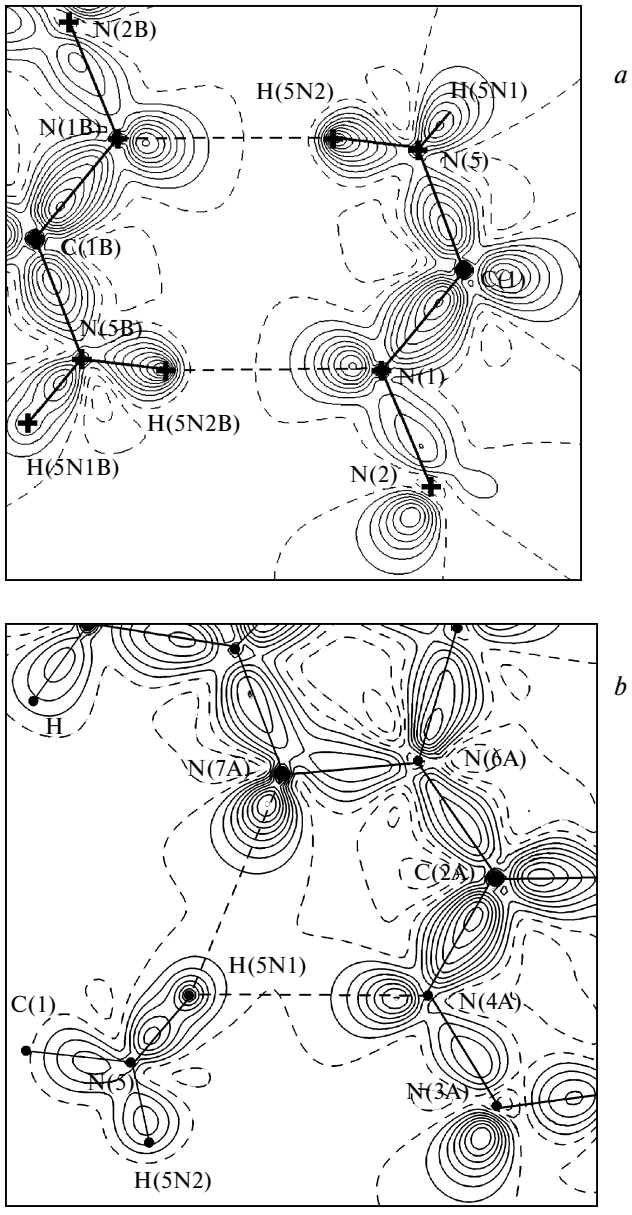

Fig. 4. Deformation electron density maps in the region of N—H...N bonds for a fragment of the centrosymmetric dimer (*a*) and the bifurcated hydrogen bond (*b*).The maps are contoured at 0.1 e Å^{-3} intervals. The negative and zero contours are dashed.

Table 3. Topological characteristics $\rho(\mathbf{r})$ at CPs (3,−1) in **1** calculated by the quantum-chemical method at the B3LYP/6-311G** level and determined by X-ray diffraction

Bond	Calculation			Experiment		
	$\rho(\mathbf{r})$ /e·Å^{-3}	$-\nabla^2\rho(\mathbf{r})$ /e·Å^{-5}	ε	$\rho(\mathbf{r})$ /e·Å^{-3}	$-\nabla^2\rho(\mathbf{r})$ /e·Å^{-5}	ε
N(1)—N(2)	2.687	20.32	0.08	2.551	5.57	0.07
N(3)—N(4)	2.742	21.28	0.08	2.694	9.26	0.04
C(1)—N(1)	2.316	25.93	0.14	2.562	22.70	0.22
C(1)—N(3)	2.345	26.39	0.15	2.433	22.20	0.18
C(1)—N(5)	2.210	24.15	0.17	2.381	25.49	0.21
C(2)—N(4)	2.342	25.71	0.19	2.587	23.62	0.24
C(2)—N(2)	2.371	25.60	0.22	2.555	24.24	0.22
C(2)—N(6)	2.029	21.72	0.15	2.054	20.29	0.29
N(6)—N(7)	2.348	14.46	0.12	2.378	5.25	0.07
C(5)—N(6)	1.988	15.40	0.15	2.136	17.59	0.10
C(3)—N(7)	2.374	20.79	0.22	2.333	20.59	0.24
C(3)—C(4)	1.974	18.27	0.20	2.148	18.69	0.21
C(4)—C(5)	2.161	21.51	0.31	2.122	17.69	0.22

indicative of a greater electron density accumulation at the lone pair of the N(1) atom, which is, apparently, associated with its polarization due to hydrogen bonding.

To the contrary, the linear arrangement of the hydrogen atom and the nitrogen lone pair in the region of the bifurcated bond is observed only for the N(5)—H(5N1)...N(7A) interaction (Fig. 4, *b*). The height and degree of polarization of the DED maximum corresponding to the lone pair of the N(7A) atom differ from the analogous characteristics for N(4A). The observed deformation electron density distribution suggests that, in spite of the shorter N(5)...N(4) distance, the contact with the pyrazole nitrogen atom is forced.

The topological analysis of $\rho(\mathbf{r})$ revealed the critical points (CP) (3,−1) for all chemical bonds and the critical points (3,+1) for two rings (pyrazole and tetrazine). A comparison of the topological characteristics at CPs (3,−1) in the isolated molecule **1** and in the crystal revealed small differences in the electron density and ellipticity (ε) at these points (Table 3). These differences are to a large extent determined by the differences in the geometry of the isolated molecule and the molecule in the crystal (see above). For example, an elongation of the C(1)—N(5) bond with the amino group in the isolated molecule reflects the weakening of conjugation, resulting in a decrease in the ellipticity ε.

The most considerable differences in the topological characteristics of $\rho(\mathbf{r})$ at CPs (3,−1) in the crystal and in the isolated molecule are observed for the N—N bonds in the tetrazine and pyrazole rings. It should be noted that the ellipticities and electron densities differ only slightly, whereas the Laplacian of the electron density $\nabla^2\rho(\mathbf{r})$ in the crystal is more than half as large (in magnitude) as that in the isolated molecule. The difference in $\nabla^2\rho(\mathbf{r})$ at CPs (3,−1) for the C—N and C—C bonds are insignificant and can be attributed to the changes in the bond lengths.

The values of $\nabla^2\rho(\mathbf{r})$ at CPs (3,−1) for the N—N bonds in **1** remain virtually unchanged with changes in the parameters of the radial functions used in the multipole refinement. Analogous discrepancies in $\nabla^2\rho(\mathbf{r})$ for homopolar bonds have been observed earlier, and they have been most comprehensively studied for the O—O bonds. It has been demonstrated[15] that quantum-chemical calculations systematically underestimate $\nabla^2\rho(\mathbf{r})$ at CP (3,−1), thus overestimating electron sharing upon the O—O bond formation. A change in the polarity of the medium leads not only to an increase in $\nabla^2\rho(\mathbf{r})$ but also to a change in its sign to positive.

Since analogous problems have been observed for other homopolar bonds formed by second-period elements, for example, for F—F (see Ref. 15 and references cited therein), it cannot be ruled out that the differences in $\nabla^2\rho(\mathbf{r})$ at CPs (3,−1) of the N—N bonds in compound **1** are associated with the influence of the crystal environment rather than are a consequence of the systematic error introduced by the multipole model.

The topological analysis of $\rho(\mathbf{r})$ in the crystal of **1** in the region of intermolecular contacts also revealed the critical points (3,−1) (Table 4) for the N—H...N bonds, stacking interactions, and C—H...N contacts listed in Table 2. The bond paths and/or CPs (3,−1) were not observed for other intermolecular contacts, including contacts in the dimer formed through stacking interactions. In the region of the presumably bifurcated N—H...N bond, two CPs (3,−1) for the H(5N(1))....N(4A) and H(5N(1))...N(7A) contacts were localized. Analogous results were obtained for the isolated dimer **B**, in which the differences in the strength of H...N interactions, according to the geometric criteria (see above), are more pronounced. Apparently, the stability of the bifurcated N—H...N bond in the crystal differs from that in the isolated molecule. For example, the minimum distance between CP (3,−1) of the N...H bonds and CP (3,+1) of the five-membered H-bonded ring is 0.55 Å, whereas this distance in the isolated dimer decreases to 0.24 Å. Such a short distance between CPs (3,−1) and (3,+1) indicates that further distortion of the molecule as the N(5)H(5N(1))N(7A) angle approaches 180° will lead to coalescence of two types of CPs, (3,−1) and (3,+1), and, as a consequence, to a change from the bifurcated-type N—H...N interaction to the usual two-center interaction.

Since the H(5N(1)) atom is involved in two (rather than in one) hydrogen bonds, it is reasonable that each component of the bifurcated H bond is, in sum, weaker, than the two-center H(5N(2))...N(1B) interaction. However, a comparison of the topological characteristics at CPs (3,−1) of the H(5N(2))...N(1B) and H(5N(1))...N(7A) hydrogen bonds demonstrated that they are virtually equal.

Table 4. Topological characteristics at CPs (3,−1) of intermolecular interactions and their energies in the crystal of **1** determined by X-ray diffraction

Fragment (symmetry code)	$\rho(\mathbf{r})$ /e·Å^{-3}	$\nabla^2\rho(\mathbf{r})$ /e·Å^{-5}	$-v(\mathbf{r})$	$h_e(\mathbf{r})$	E /kcal mol^{-1}
			Hartree Å^{-3}		
	Interactions N—H....N				
N(5)—H(5N(2))...N(1B) $(1-x, -y, -z)$	0.129	0.62	0.0676	−0.0121	3.14
N(5)—H(5N(1))...N(4A) $(1-x, -0.5+y, 0.5-z)$	0.094	1.47	0.0656	0.0187	3.05
	(0.055)[a]	(0.786)[a]	(0.034)[a]	(0.0097)[a]	(−1.57)[a]
N(5)—H(5N(1))...N(7A) $(1-x, -0.5+y, 0.5-z)$	0.132	0.91	0.0762	−0.0064	3.54
	(0.175)[a]	(1.58)[a]	(0.115)[a]	(−0.0013)[a]	(5.33)[a]
	Interactions C—H...N				
N(3)...H(61)—C(6) $(1-x, -0.5+y, 0.5-z)$	0.039	0.79	0.0255	0.0148	1.19
N(3)...H(72)—C(7) $(x, 0.5-y, 0.5+z)$	0.050	0.80	0.0298	0.0133	1.39
N(2)...H(62)—C(6) $(-x, 1-y, -z)$	0.043	0.67	0.0243	0.0115	1.13
	Stacking interactions				
C(1)...C(4) $(1-x, 1-y, -z)$	0.040	0.46	0.0182	0.0069	0.85
C(5)...N(4) $(1-x, 1-y, -z)$	0.036	0.42	0.0159	0.0066	0.74

[a] The value is calculated by the PBE/TZ2P//B3LYP/6-311+G** method for the dimer **B** dimer stabilized by the bifurcated N—H...N bond.

Moreover, both these interactions, unlike the second component of the bifurcated bond, as well as of all other intermolecular contacts in the crystal of **1**, are characterized by the negative energy density, $h_e(r)$ and, consequently, correspond to an intermediate type of interatomic interactions. Quantum-chemical calculations demonstrated that the intermediate type of interactions is observed for the H(5N(1))...N(7) hydrogen bond in the isolated dimer **B** as well.

To estimate the strength of interatomic interactions, we used the correlation between the potential energy density ($v(r)$) and the contact energy.[6] The lowest contact energies (1.13—1.39 kcal mol^{-1}) were observed for the C—H...N interactions. Although the energies of the C(1)...C(4A) and C(5)...N(4A) interactions are also low (0.74—0.85 kcal mol^{-1}), the total energy of the dimer stabilized by a stacking interaction (3.18 kcal mol^{-1}) is twice as high as the energy of the C—H...N interactions. The latter value is virtually equal to the energy of the N(5)—H(5N(2))...N(1B) hydrogen bond (3.14 kcal mol^{-1}) through which molecules **1** are linked into the centrosymmetric dimer **A**; the energy of the latter is 6.28 kcal mol^{-1}. The energy of the dimer **B** formed through the bifurcated hydrogen bond is even slightly higher (6.59 kcal mol^{-1}). The energy of the N(5)—H(5N(1))...N(7A) interaction (3.54 kcal mol^{-1}) is slightly higher than the energy of the two-center N(5)—H(5N(2))...N(1B) bond.

Taking into account all the above-mentioned interactions, the total energy of intermolecular contacts per molecule in the crystal of **1** is 19.5 kcal mol^{-1}, which is typical of the sublimation energies of organic compounds.[16] In turn, the crystal lattice energy, which was estimated from the energy of intermolecular contacts, is 78 kcal mol^{-1}.

Interestingly, although the energies of the N(5)—H(5N(1))...N(4A) and N(5)—H(5N(1))...N(7A) interactions (1.57 and 5.33 kcal mol^{-1}, respectively) in the isolated dimer **B** differ substantially from the corresponding energies in the crystal, the total energy of the bifurcated bond in the crystal is virtually equal to that in the isolated dimer (6.90 kcal mol^{-1}). Moreover, as can be seen from Table 4, the sums of the values of $\rho(\mathbf{r})$ and $\nabla^2\rho(\mathbf{r})$ at CPs (3,−1) for the N(5)—H(5N(1))...N(4A) and N(5)—H(5N(1))...N(7A) interactions in the crystal (2.226 e Å^{-3} and 2.38 e Å^{-5}) are nearly equal to those in the isolated dimers **B** (2.230 e Å^{-3} and 2.37 e Å^{-5}, respectively).

The results of the present study demonstrate the advantages of high-resolution X-ray diffraction analysis in studies of bifurcated hydrogen bonds. This method allows one not only to determine the nature of interactions, but also to estimate their energies. In contrast to the two-center H bonds, the total energy of the bifurcated N—H...N interaction in molecule **1** is virtually independent of the geometric parameters of two contacts and is determined exclusively by the nature of the interacting atoms.

Experimental

Compound **1** ($C_7H_9N_7$, M = 191.21) was synthesized according to a known procedure.[17] Orange monoclinic crystals were grown from a toluene solution, space group $P2_1/c$, $a = 6.8748(2)$, $b = 10.3652(3)$, $c = 12.6856(4)$ Å, $\beta = 104.183(1)°$,

V = 876.40(5) Å^3, Z = 4, d_{calc} = 1.449 g cm^{-3}, μ(Mo-Kα) = 1.02 cm^{-1}, $F(000)$ = 400. The intensities of 25768 reflections were measured at 110 K on a Smart 1000 CCD diffractometer (λ(Mo-Kα) = 0.71072 Å, ω scanning technique with a step of 0.3°, exposure time per frame was 10 s, 2θ < 80°); 5297 independent reflections (R_{int} = 0.0604) were used in the refinement. The X-ray diffraction data were processed and merged using the SAINT Plus [18] and SADABS[19] program packages.

The structure was solved by direct methods with the use of successive electron density maps. All hydrogen atoms were located from difference electron density maps. The structure was refined against F^2_{hkl} with anisotropic displacement parameters for all nonhydrogen atoms and isotropic displacement parameters for hydrogen atoms.

The final R factors for **1** were as follows: R_1 = 0.0459 (calculated based on F_{hkl} for 4012 reflections with $I > 2\sigma(I)$), wR_2 = 0.1230 (calculated based on F^2_{hkl} for all 5297 reflections); the number of parameters in the refinement was 163, GOOF = 0.971. The calculations were carried out using the SHELXTL 5.10 program package.[20]

The experimental electron density function was determined in the analytical form by the multipole refinement of X-ray diffraction data in terms of the Hansen—Coppens model[21] using the XD program package.[22] In the multipole refinement, the coordinates, anisotropic displacement parameters, and the multipole parameters up to the octupole level (l = 3) were refined for all nonhydrogen atoms against F_{hkl}. The positions of the hydrogen atoms and their isotropic displacement parameters remained fixed. Before the refinement, all C—H distances were normalized to the ideal distance (1.08 Å). The N—H distances were calculated by the quantum-chemical method (B3LYP/6-311G**). In the multipole refinement, the H atoms were refined up to the dipole level (l = 2) taking into account the cylindrical symmetry. The correctness of the anisotropic atomic displacement parameters was estimated using the Hirshfeld test,[23] which was at most $6 \cdot 10^{-4}$ Å^2 for the bonds. The results of the multipole refinement are characterized by the following parameters: R = 0.0303, wR = 0.0337, GOOF = 0.758 for 3935 reflections with $I > 3\sigma(I)$. The residual electron density ($\rho(\mathbf{r})_{exp} - \rho(\mathbf{r})_{mult}$) was at most 0.16 e Å^{-3}.

The potential energy density ($\nu(\mathbf{r})$) was calculated from X-ray diffraction data using an approximation in terms of the Thomas—Fermi theory.[24] According to this approach, the kinetic energy density ($g(\mathbf{r})$) can be calculated from the equation

$$g(\mathbf{r}) = (3/10)(3\pi^2)^{2/3}[\rho(\mathbf{r})]^{5/3} + (1/72)|\nabla\rho(\mathbf{r})|^2/\rho(\mathbf{r}) + \\ + 1/6\nabla^2\rho(\mathbf{r}),$$

combined with the local virial theorem[5] ($2g(\mathbf{r}) + \nu(\mathbf{r}) = 1/4\nabla^2\rho(\mathbf{r})$), which allows calculations of both the potential energy density and the local electron energy density ($h_e(\mathbf{r})$). The CPs (3,−1) were found and the corresponding topological characteristics, including $h_e(\mathbf{r})$, $g(\mathbf{r})$, and $\nu(\mathbf{r})$, were calculated using the WINXPRO 1.5.20 program.[25]

Quantum-chemical calculations for molecule **1** were performed using the Gaussian 98 program[26] with the B3LYP functional and the 6-31+G** basis set. The geometry optimization of the N—H...N-bonded dimer **B** was carried out using the PRIRODA program[27] (PBE/TZ2P). The electron density function was determined from the results of B3LYP/6-311G** calculations using the geometry calculated at the PBE/TZ2P level of theory. The topological analysis of the calculated function $\rho(\mathbf{r})$ was performed using the MORPHY 98 program.[28]

This study was financially supported by the Russian Foundation for Basic Research (Project No. 03-03-32214) and the Foundation of the President of the Russian Federation (Federal Programs for the Support of Leading Scientific Schools, Grant NSh 1060.2003.03, and the Program for Support of Young Doctors, Grant MK-1209.2003.03).

References

1. K. A. Lyssenko, I. L. Odinets, P. V. Kazakov, M. P. Pasechnik, and M. Yu. Antipin, *Izv. Akad. Nauk, Ser. Khim.*, 2005, 553 [*Russ. Chem. Bull., Int. Ed.*, 2005, **54**, 560].
2. G. A. Jeffrey and W. Saenger, *Hydrogen Bonding in Biological Structures*, Springer-Verlag, Berlin, 1991.
3. (a) A. V. Iogansen, *Spectrochimica Acta*, 1999, **A55**, 1585; (b) L. M. Epstein and E. S. Shubina, *Coord. Chem. Rev.*, 2002, **231**, 165.
4. T. Steiner, *Angew. Chem., Int. Ed.*, 2002, **41**, 58.
5. R. F. W. Bader, *Atoms in Molecules. A Quantum Theory*, Clarendron Press, Oxford, 1990.
6. E. Espinosa, E. Mollins, and C. Lecomte, *Chem. Phys. Lett.*, 1998, **285**, 170.
7. I. Rozas, I. Alkorta, and J. Elguero, *J. Phys. Chem. A*, 1998, **102**, 9925.
8. R. S. Gopalan, G. U. Kulkarni, E. Subramanian, and S. Renganayaki, *J. Mol. Struct.*, 2000, **524**, 169.
9. J. Ellena, A. E. Goeta, J. A. K. Howard, and G. Punte, *J. Phys. Chem. A*, 2001, **105**, 8696.
10. D. E. Chavez, M. A. Hiskey, and R. D. Gilardi, *Angew. Chem., Int. Ed.*, 2000, **39**, 1791.
11. C. Glidewell, P. Lightfoot, B. J. L. Royles, and D. M. Smith, *J. Chem. Soc., Perkin Trans. 2*, 1997, 1167.
12. A. Klein, E. J. L. McInnes, T. Scheiring, and S. Zalis, *J. Chem. Soc., Faraday Trans.*, 1998, **94**, 2979.
13. *Cambridge Crystallographic Database*, release 2003.
14. M. Yu. Antipin, T. V. Timofeeva, D. S. Yufit, and J. Sauer, *Izv. Akad. Nauk, Ser. Khim.*, 1995, 2443 [*Russ. Chem. Bull.*, 1995, **44**, 2337 (Engl. Transl.)].
15. K. A. Lyssenko, M. Yu. Antipin, and V. N. Khrustalev, *Izv. Akad. Nauk, Ser. Khim.*, 2001, 1465 [*Russ. Chem. Bull., Int. Ed.*, 2001, **50**, 1539].
16. J. Bernstein, *Polymorphism in Molecular Crystals*, Clarendon Press, Oxford, 2002.
17. M. D. Coburn, G. A. Buntain, B. W. Harris, M. A. Hiskey, K.-Y. Lee, and D. G. Ott, *J. Heterocyclic Chem.*, 1991, **28**, 2049.
18. *SMART. Bruker Molecular Analysis Research Tool*, v. 5.059, 1998, Bruker AXS, Madison, Wisconsin, USA.
19. G. M. Sheldrick, *SADABS*, Bruker AXS Inc., Madison, WI-53719, USA, 1997.
20. G. M. Sheldrick, *SHELXTL-97*, Version 5.10, Bruker AXS Inc., Madison, WI-53719, USA, 1998.
21. N. K. Hansen and P. Coppens, *Acta Crystallogr.*, 1978, **A34**, 909.

22. T. Koritsanszky, S. T. Howard, T. Richter, P. Macchi, A. Volkov, C. Gatti, P. R. Mallinson, L. J. Farrugia, Z. Su, and N. K. Hansen, *XD — A Computer Program Package for Multipole Refinement and Topological Analysis of Charge Densities from Diffraction Data*, 2003.
23. F. L. Hirshfeld, *Acta Crystallogr.*, 1976, **A32**, 239.
24. D. A. Kirzhnitts, *Zh. Eksp. Teor. Fiz.*, 1957, **5**, 64 [*J. Exp. Theor. Phys. USSR*, 1957, **5**, 64 (Engl. Transl.)].
25. A. Stash and V. Tsirelson, *WinXPRO — a Program for Calculation of the Crystal and Molecular Properties Using the Model Electron Density*, Moscow (Russia), 2001. A further information available at http://xray.nifhi.ru/wxp/
26. M. J. Frisch, G. W. Trucks, H. B. Schlegel, G. E. Scuseria, M. A. Robb, J. R. Cheeseman, V. G. Zakrzewski, J. A. Montgomery, Jr., R. E. Stratmann, J. C. Burant, S. Dapprich, J. M. Millam, A. D. Daniels, K. N. Kudin, M. C. Strain, O. Farkas, J. Tomasi, V. Barone, M. Cossi, R. Cammi, B. Mennucci, C. Pomelli, C. Adamo, S. Clifford, J. Ochterski, G. A. Petersson, P. Y. Ayala, Q. Cui, K. Morokuma, D. K. Malick, A. D. Rabuck, K. Raghavachari, J. B. Foresman, J. Cioslowski, J. V. Ortiz, A. G. Baboul, B. B. Stefanov, G. Liu, A. Liashenko, P. Piskorz, I. Komaromi, R. Gomperts, R. L. Martin, D. J. Fox, T. Keith, M. A. Al-Laham, C. Y. Peng, A. Nanayakkara, M. Challacombe, P. M. W. Gill, B. Johnson, W. Chen, M. W. Wong, J. L. Andres, C. Gonzalez, M. Head-Gordon, E. S. Replogle, and J. A. Pople, *Gaussian 98*, *Revision A.9*, Gaussian, Inc., Pittsburgh PA, 1998.
27. D. N. Laikov, *Chem. Phys. Lett.*, 1997, **281**, 151.
28. (a) *MORPHY98*, *A Topological Analysis Program Written* by P. L. A. Popelier with a Contribution from R. G. A. Bone (UMIST, Engl, EU); (b) P. Popelier, *Chem. Phys. Lett.*, 1994, **228**, 160.

Received October 7, 2004;
in revised form November 25, 2004